

# Development of discontinuous Galerkin solver for high order computation of hypersonic Shock-Boundary Layer Interaction (SBLI)

Potluri Vachan Deep  
IIT Bombay

Supervisors: Profs. Bhalchandra Puranik and Kowsik Bodi

## Need for high order hypersonic CFD simulations

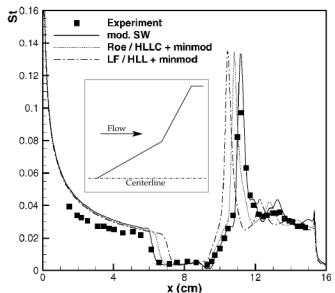
Issues in hypersonic CFD [Can15; CMT09; Gai15; Kni+12; Kni+17]

- ▶ Reliable modelling of finite rate chemistry & turbulence
- ▶ Surface heat transfer sensitivity to grid and numerical details

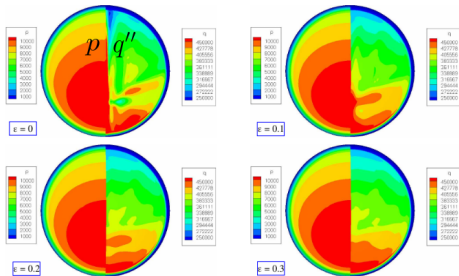
# Need for high order hypersonic CFD simulations

Issues in hypersonic CFD [Can15; CMT09; Gai15; Kni+12; Kni+17]

- Reliable modelling of finite rate chemistry & turbulence
- Surface heat transfer sensitivity to grid and numerical details



(a) Variation with flux scheme [DCN05]



(b) Variation with a flux scheme parameter  $\varepsilon$  [CMT09]

Figure: Sensitivity of surface heat transfer

# Need for high order hypersonic CFD simulations

Issues in hypersonic CFD [Can15; CMT09; Gai15; Kni+12; Kni+17]

- ▶ Reliable modelling of finite rate chemistry & turbulence
- ▶ Surface heat transfer sensitivity to grid and numerical details
  - 💡 Adaptive meshing techniques
  - 💡 High order methods

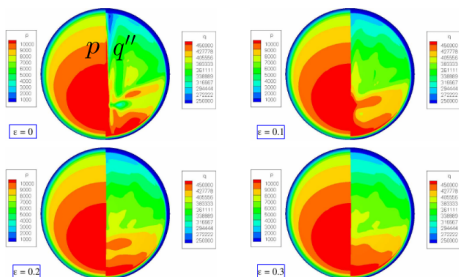
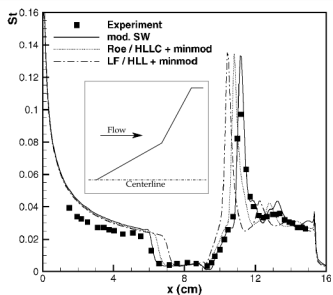


Figure: Sensitivity of surface heat transfer

# Need for high order hypersonic CFD simulations

## Issues in hypersonic CFD [Can15; CMT09; Gai15; Kni+12; Kni+17]

- ▶ Reliable modelling of finite rate chemistry & turbulence
- ▶ Surface heat transfer sensitivity to grid and numerical details
  - 💡 Adaptive meshing techniques
  - 💡 High order methods
- ▶ Efforts using FVM and FDM
  - Adaptive mesh refinement [Fra+12; Gre+10; SNC14]
  - Compact FD schemes [LD07; Maw+06; Zha+11], and WENO FV schemes [SZH10]

# Need for high order hypersonic CFD simulations

## Issues in hypersonic CFD [Can15; CMT09; Gai15; Kni+12; Kni+17]

- ▶ Reliable modelling of finite rate chemistry & turbulence
- ▶ Surface heat transfer sensitivity to grid and numerical details
  - 💡 Adaptive meshing techniques
  - 💡 High order methods
- ▶ Efforts using FVM and FDM
  - Adaptive mesh refinement [Fra+12; Gre+10; SNC14]
  - Compact FD schemes [LD07; Maw+06; Zha+11], and WENO FV schemes [SZH10]
- ▶ A newly emerging alternative: DG [CKS12; HW07]
  - ✓ Compact cell-local interpolation
    - High order computations without increase in algorithm's complexity
    - Suitable to *hp*-adaptation and parallel computing
  - ! Limiters for hypersonic flows

## Only few high order hypersonic FEM/DG simulations in the past decade

- ▶ Streamwise Upwind Petrov Galerkin method  
[Hol+18; KC10; Kir+14]
- ▶ Adaptive Edge-based FEM [Gao+19; Seg+19]
- ▶  $rp$ -adaptive DG method [BRG13]
- ▶ Smooth PDE-based artificial viscosity DG limiter  
[BD10; BM12; BM13; Chi+19]

## Only few high order hypersonic FEM/DG simulations in the past decade

- ▶ Streamwise Upwind Petrov Galerkin method  
[Hol+18; KC10; Kir+14]
  - ▶ Adaptive Edge-based FEM [Gao+19; Seg+19]
  - ▶  $r\mu$ -adaptive DG method [BRG13]
  - ▶ Smooth PDE-based artificial viscosity DG limiter  
[BD10; BM12; BM13; Chi+19]
- Most use linear polynomial basis

# Only few high order hypersonic FEM/DG simulations in the past decade

- ▶ Streamwise Upwind Petrov Galerkin method [Hol+18; KC10; Kir+14]
- ▶ Adaptive Edge-based FEM [Gao+19; Seg+19]
- ▶  $rp$ -adaptive DG method [BRG13]
- ▶ Smooth PDE-based artificial viscosity DG limiter [BD10; BM12; BM13; Chi+19]

Only few show high order results

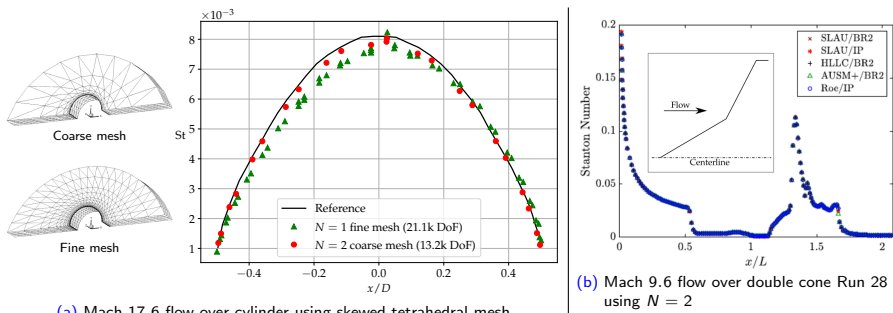


Figure: Surface heat transfer results from [Chi+19]

### Aim

To develop a DG high order simulation framework for hypersonic flows

### Summary of work done in the past year

- ① A DG solver for compressible flows using a subcell limiter algorithm has been developed
- ② An extension to hypersonic regime has been proposed and tested

# Numerical method

Basic idea of the DG limiter: FV subcell equivalence [Hen+21]

$$J \frac{\partial \mathbf{U}}{\partial t} + \frac{\partial \mathbf{F}}{\partial \xi} = \mathbf{0}$$

1d Euler equations in reference space

$$\mathbf{U}(\xi, t) \approx \sum_{i=0}^N \mathbf{U}_i(t) \ell_i(\xi), \quad \mathbf{F}(\xi, t) \approx \sum_{i=0}^N \mathbf{F}(\mathbf{U}_i(t)) \ell_i(\xi) \quad \text{Approximation}$$

$$- J \dot{\mathbf{U}}_i = \sum_{j=0}^N [D_{ij} \mathbf{F}_j] + (\text{surface term}) \coloneqq R_{\text{std}}(\mathbf{F})_i \quad \text{Co-located Galerkin discretisation}$$

$$\sum_{j=0}^N D_{ij} \mathbf{F}_j = \frac{\widehat{\mathbf{F}}_{i+1} - \widehat{\mathbf{F}}_i}{\widehat{\xi}_{i+1} - \widehat{\xi}_i} \quad \text{FV subcell equivalence (flux reconstruction)}$$

# Numerical method

Basic idea of the DG limiter: FV subcell equivalence [Hen+21]

$$J \frac{\partial \mathbf{U}}{\partial t} + \frac{\partial \mathbf{F}}{\partial \xi} = 0$$

1d Euler equations in reference space

$$\mathbf{U}(\xi, t) \approx \sum_{i=0}^N \mathbf{U}_i(t) \ell_i(\xi), \quad \mathbf{F}(\xi, t) \approx \sum_{i=0}^N \mathbf{F}(\mathbf{U}_i(t)) \ell_i(\xi) \quad \text{Approximation}$$

$$- J \dot{\mathbf{U}}_i = \sum_{j=0}^N [D_{ij} \mathbf{F}_j] + (\text{surface term}) := R_{\text{std}}(\mathbf{F})_i \quad \text{Co-located Galerkin discretisation}$$

$$\sum_{j=0}^N D_{ij} \mathbf{F}_j = \frac{\widehat{\mathbf{F}}_{i+1} - \widehat{\mathbf{F}}_i}{\widehat{\xi}_{i+1} - \widehat{\xi}_i}$$

FV subcell equivalence (flux reconstruction)

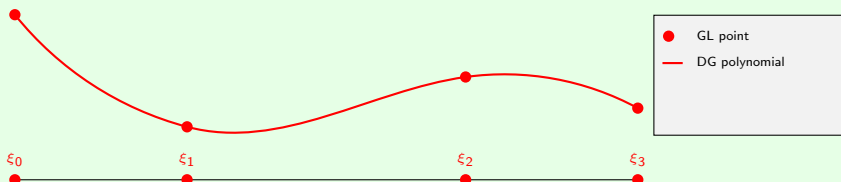


Figure: Cubic ( $N = 3$ ) DG element in reference space

# Numerical method

Basic idea of the DG limiter: FV subcell equivalence [Hen+21]

$$J \frac{\partial \mathbf{U}}{\partial t} + \frac{\partial \mathbf{F}}{\partial \xi} = 0$$

1d Euler equations in reference space

$$\mathbf{U}(\xi, t) \approx \sum_{i=0}^N \mathbf{U}_i(t) \ell_i(\xi), \quad \mathbf{F}(\xi, t) \approx \sum_{i=0}^N \mathbf{F}(\mathbf{U}_i(t)) \ell_i(\xi)$$

Approximation

$$- J \dot{\mathbf{U}}_i = \sum_{j=0}^N [D_{ij} \mathbf{F}_j] + (\text{surface term}) := R_{\text{std}}(\mathbf{F})_i$$

Co-located Galerkin discretisation

$$\sum_{j=0}^N D_{ij} \mathbf{F}_j = \frac{\widehat{\mathbf{F}}_{i+1} - \widehat{\mathbf{F}}_i}{\widehat{\xi}_{i+1} - \widehat{\xi}_i}$$

FV subcell equivalence (flux reconstruction)

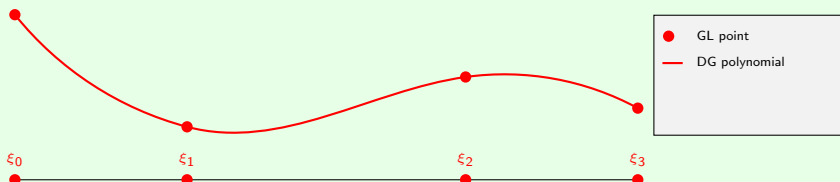


Figure: Cubic ( $N = 3$ ) DG element in reference space

# Numerical method

Basic idea of the DG limiter: FV subcell equivalence [Hen+21]

$$J \frac{\partial \mathbf{U}}{\partial t} + \frac{\partial \mathbf{F}}{\partial \xi} = 0$$

1d Euler equations in reference space

$$\mathbf{U}(\xi, t) \approx \sum_{i=0}^N \mathbf{U}_i(t) \ell_i(\xi), \quad \mathbf{F}(\xi, t) \approx \sum_{i=0}^N \mathbf{F}(\mathbf{U}_i(t)) \ell_i(\xi)$$

Approximation

$$- J \dot{\mathbf{U}}_i = \sum_{j=0}^N [D_{ij} \mathbf{F}_j] + (\text{surface term}) \coloneqq R_{\text{std}}(\mathbf{F})_i$$

Co-located Galerkin discretisation

$$\sum_{j=0}^N D_{ij} \mathbf{F}_j = \frac{\widehat{\mathbf{F}}_{i+1} - \widehat{\mathbf{F}}_i}{\widehat{\xi}_{i+1} - \widehat{\xi}_i}$$

FV subcell equivalence (flux reconstruction)

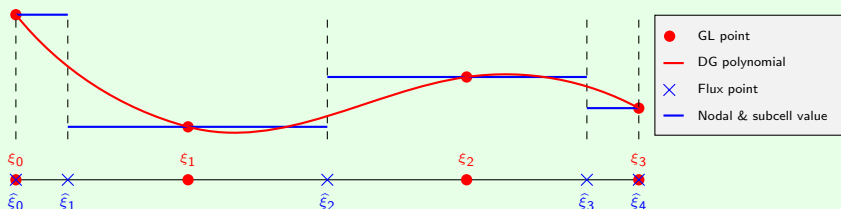
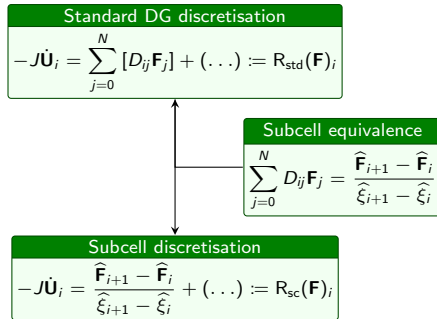
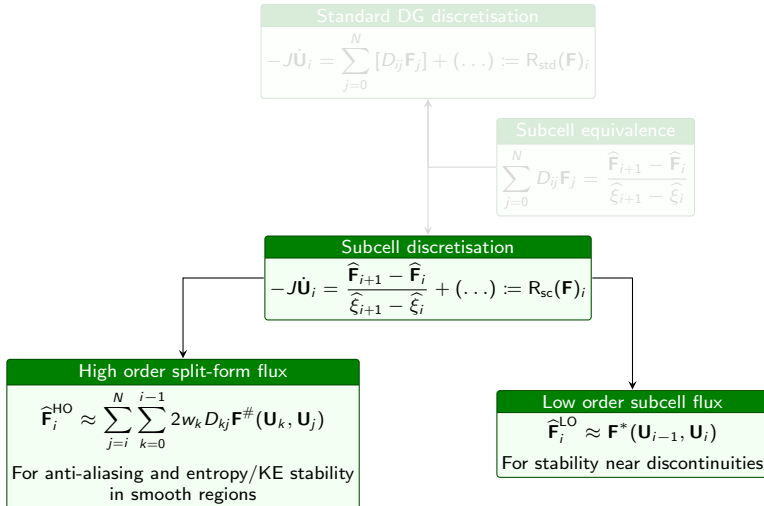


Figure: Cubic ( $N = 3$ ) DG element in reference space

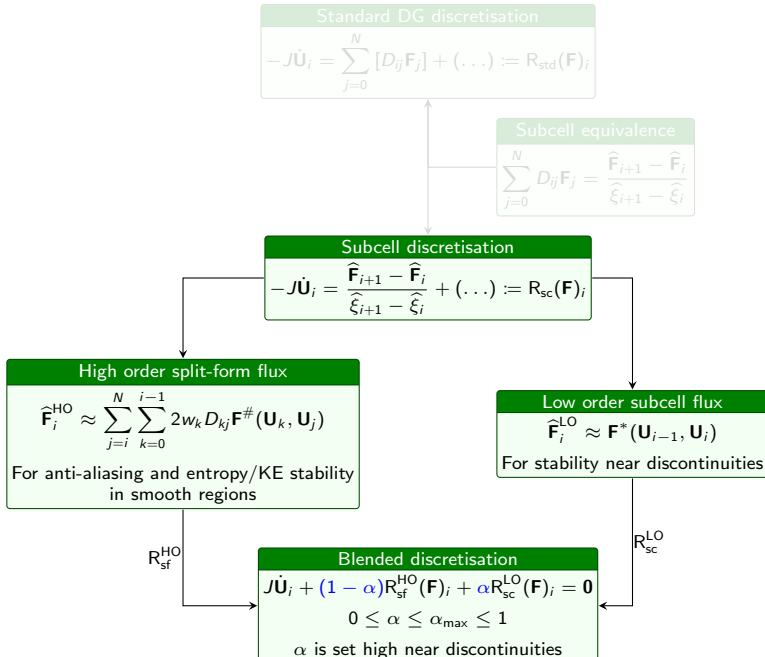
## Limiting for inviscid flows



## Limiting for inviscid flows



# Limiting for inviscid flows



## Extention to compressible NS equations: DG-BR1 approach [Boh+20]

$$J\mathbf{Z} + \frac{\partial(-\mathbf{U})}{\partial\xi} = \mathbf{0}$$

$$J\frac{\partial\mathbf{U}}{\partial t} + \frac{\partial\mathbf{F}_a(\mathbf{U})}{\partial\xi} + \frac{\partial\mathbf{F}_d(\mathbf{U}, \mathbf{Z})}{\partial\xi} = \mathbf{0}$$

## Extention to compressible NS equations: DG-BR1 approach [Boh+20]

$$J\mathbf{Z} + \frac{\partial(-\mathbf{U})}{\partial\xi} = \mathbf{0}$$

$$J\frac{\partial\mathbf{U}}{\partial t} + \frac{\partial\mathbf{F}_a(\mathbf{U})}{\partial\xi} + \frac{\partial\mathbf{F}_d(\mathbf{U}, \mathbf{Z})}{\partial\xi} = \mathbf{0}$$

$$J\mathbf{Z}_i - \mathbf{R}_{\text{std}}(\mathbf{U})_i = \mathbf{0}$$

$$J\dot{\mathbf{U}}_i + \left[ (1 - \alpha)\mathbf{R}_{\text{sf}}^{\text{HO}}(\mathbf{F}_a)_i + \alpha\mathbf{R}_{\text{sc}}^{\text{LO}}(\mathbf{F}_a)_i \right] + \mathbf{R}_{\text{std}}(\mathbf{F}_d)_i = \mathbf{0}$$

## Extention to compressible NS equations: DG-BR1 approach [Boh+20]

$$J\mathbf{Z} + \frac{\partial(-\mathbf{U})}{\partial\xi} = \mathbf{0}$$

$$J\frac{\partial\mathbf{U}}{\partial t} + \frac{\partial\mathbf{F}_a(\mathbf{U})}{\partial\xi} + \frac{\partial\mathbf{F}_d(\mathbf{U}, \mathbf{Z})}{\partial\xi} = \mathbf{0}$$

$$J\mathbf{Z}_i - R_{\text{std}}(\mathbf{U})_i = \mathbf{0}$$

$$J\dot{\mathbf{U}}_i + \left[ (1 - \alpha) R_{\text{sf}}^{\text{HO}}(\mathbf{F}_a)_i + \alpha R_{\text{sc}}^{\text{LO}}(\mathbf{F}_a)_i \right] + R_{\text{std}}(\mathbf{F}_d)_i = \mathbf{0}$$

### Modification for hypersonic flows

- ① Scale diffusive flux discretisation near wall

$$J\dot{\mathbf{U}}_i + (1 - \alpha) R_{\text{sf}}^{\text{HO}}(\mathbf{F}_a)_i + \alpha R_{\text{sc}}^{\text{LO}}(\mathbf{F}_a)_i + (1 - \alpha_d) R_{\text{std}}(\mathbf{F}_d)_i = \mathbf{0}, \quad \alpha_d = \begin{cases} \alpha / \alpha_{\max} & \text{Near wall} \\ 0 & \text{Elsewhere} \end{cases}$$

## Extention to compressible NS equations: DG-BR1 approach [Boh+20]

$$J\mathbf{Z} + \frac{\partial(-\mathbf{U})}{\partial\xi} = \mathbf{0}$$

$$J\frac{\partial\mathbf{U}}{\partial t} + \frac{\partial\mathbf{F}_a(\mathbf{U})}{\partial\xi} + \frac{\partial\mathbf{F}_d(\mathbf{U}, \mathbf{Z})}{\partial\xi} = \mathbf{0}$$

$$J\mathbf{Z}_i - R_{\text{std}}(\mathbf{U})_i = \mathbf{0}$$

$$J\dot{\mathbf{U}}_i + \left[ (1-\alpha)R_{\text{sf}}^{\text{HO}}(\mathbf{F}_a)_i + \alpha R_{\text{sc}}^{\text{LO}}(\mathbf{F}_a)_i \right] + R_{\text{std}}(\mathbf{F}_d)_i = \mathbf{0}$$

### Modification for hypersonic flows

- ① Scale diffusive flux discretisation near wall

$$J\dot{\mathbf{U}}_i + (1-\alpha)R_{\text{sf}}^{\text{HO}}(\mathbf{F}_a)_i + \alpha R_{\text{sc}}^{\text{LO}}(\mathbf{F}_a)_i + (1-\alpha_d)R_{\text{std}}(\mathbf{F}_d)_i = \mathbf{0}, \quad \alpha_d = \begin{cases} \alpha/\alpha_{\max} & \text{Near wall} \\ 0 & \text{Elsewhere} \end{cases}$$

- ② For wall cells

$$\alpha'_w = \max(\alpha_w, \alpha_{\text{imposed}}), \quad \alpha_{\text{imposed}} \approx \begin{cases} 0.95\alpha_{\max} & t \leq T_w \approx 5\Delta y_w^2 / \nu_\infty \\ 0.95\alpha_{\max}(2 - t/T_w) & 1 < t/T_w \leq 2 \\ 0 & \text{Otherwise} \end{cases}$$

## Extention to compressible NS equations: DG-BR1 approach [Boh+20]

$$J\mathbf{Z} + \frac{\partial(-\mathbf{U})}{\partial\xi} = \mathbf{0}$$

$$J\frac{\partial\mathbf{U}}{\partial t} + \frac{\partial\mathbf{F}_a(\mathbf{U})}{\partial\xi} + \frac{\partial\mathbf{F}_d(\mathbf{U}, \mathbf{Z})}{\partial\xi} = \mathbf{0}$$

$$J\mathbf{Z}_i - R_{\text{std}}(\mathbf{U})_i = \mathbf{0}$$

$$J\dot{\mathbf{U}}_i + \left[ (1-\alpha)R_{\text{sf}}^{\text{HO}}(\mathbf{F}_a)_i + \alpha R_{\text{sc}}^{\text{LO}}(\mathbf{F}_a)_i \right] + R_{\text{std}}(\mathbf{F}_d)_i = \mathbf{0}$$

## Modification for hypersonic flows

- ① Scale diffusive flux discretisation near wall

$$J\dot{\mathbf{U}}_i + (1-\alpha)R_{\text{sf}}^{\text{HO}}(\mathbf{F}_a)_i + \alpha R_{\text{sc}}^{\text{LO}}(\mathbf{F}_a)_i + (1-\alpha_d)R_{\text{std}}(\mathbf{F}_d)_i = \mathbf{0}, \quad \alpha_d = \begin{cases} \alpha/\alpha_{\max} & \text{Near wall} \\ 0 & \text{Elsewhere} \end{cases}$$

- ② For wall cells

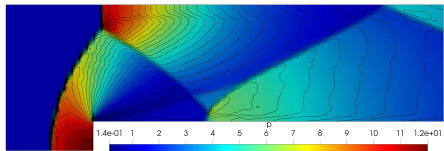
$$\alpha'_w = \max(\alpha_w, \alpha_{\text{imposed}}), \quad \alpha_{\text{imposed}} \approx \begin{cases} 0.95\alpha_{\max} & t \leq T_w \approx 5\Delta y_w^2 / \nu_\infty \\ 0.95\alpha_{\max}(2 - t/T_w) & 1 < t/T_w \leq 2 \\ 0 & \text{Otherwise} \end{cases}$$

## Other settings

- Time integration: explicit TVD-RK3 [GS98] and 5-stage LSERK4 [KCL00]
  - Local stepping used for convergence acceleration in steady simulations
- Boundary conditions: weak imposition [Men+14]

## Verification of implementation

- Solver named “PLENS” implemented in C++ using deal.II [Arn+21]

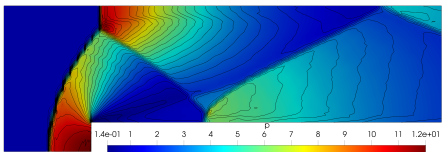


(a) Forward facing step in Mach 3 wind tunnel ( $N = 4$ )

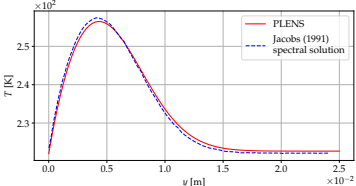
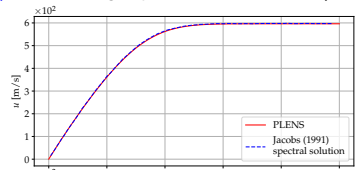
**Figure:** Supersonic cases simulated without hypersonic modification

# Verification of implementation

- Solver named “PLENS” implemented in C++ using deal.II [Arn+21]



(a) Forward facing step in Mach 3 wind tunnel ( $N = 4$ )

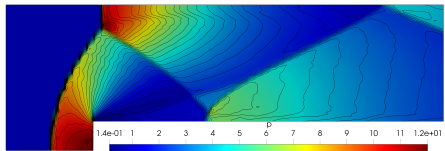


(b) Mach 2 flat plate boundary layer ( $N = 4$ )

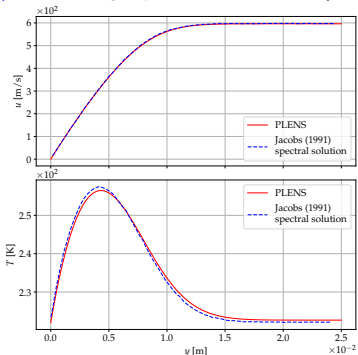
Figure: Supersonic cases simulated without hypersonic modification

# Verification of implementation

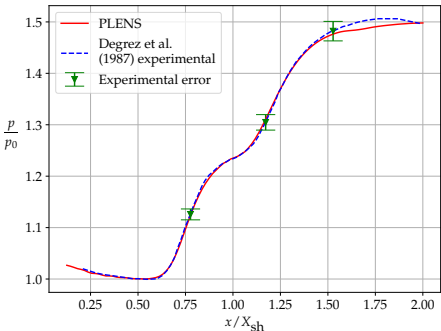
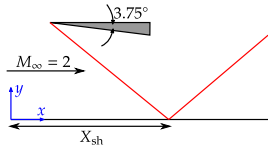
- Solver named “PLENS” implemented in C++ using deal.II [Arn+21]



(a) Forward facing step in Mach 3 wind tunnel ( $N = 4$ )



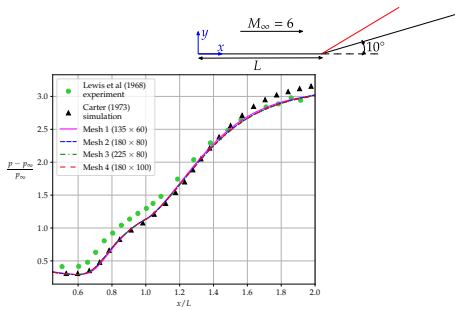
(b) Mach 2 flat plate boundary layer ( $N = 4$ )



(c) Mach 2 shock-boundary layer interaction ( $N = 4$ )

Figure: Supersonic cases simulated without hypersonic modification

# Mach 6 SBLI



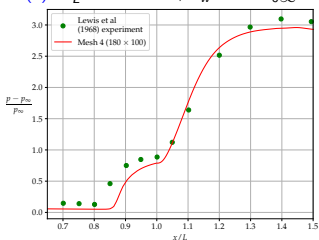
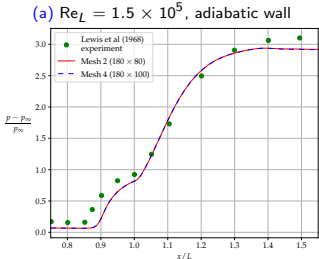
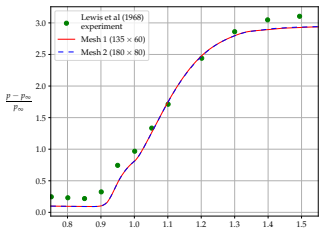
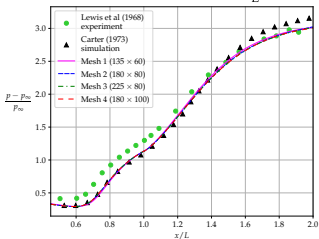
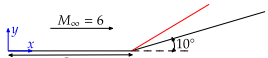
(a)  $\text{Re}_L = 1.5 \times 10^5$ , adiabatic wall

Consistent discrepancy  
with experiments

- ▶ Carter's result [Car73]
- ▶ Grid converged results  
at  $\text{Re}_L = 1.5 \times 10^5$

Using  $N = 2$

# Mach 6 SBLI



Using  $N = 2$

Consistent discrepancy with experiments

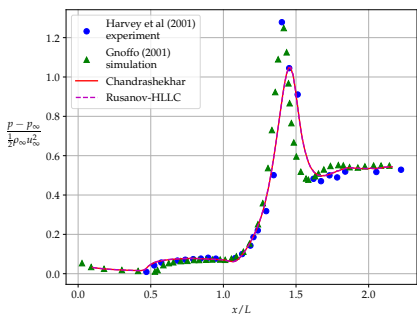
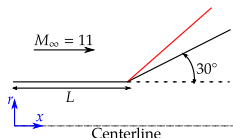
- ▶ Carter's result [Car73]
- ▶ Grid converged results at  $Re_L = 1.5 \times 10^5$  and  $3 \times 10^5$

Probably due to uncertainty in experimental arrangement and measurement

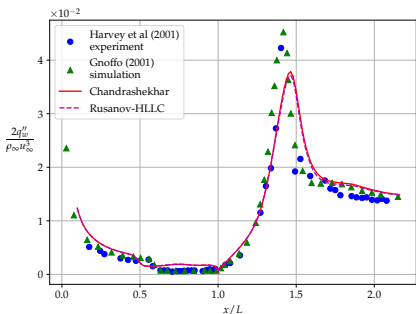
# Mach 11 SBLI (HCEF Run 9)

## ► Corase grid (using $N = 2$ )

- Separation extent over predicted
- Peak values suppressed



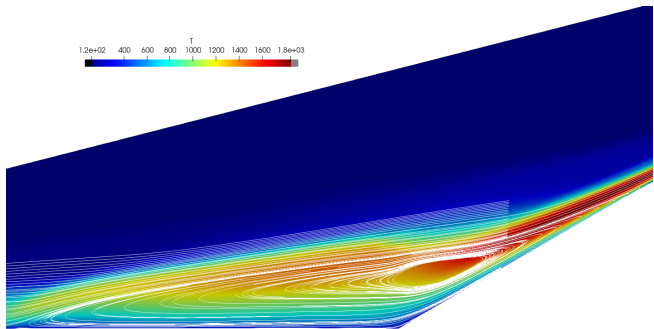
(a)  $c_p$



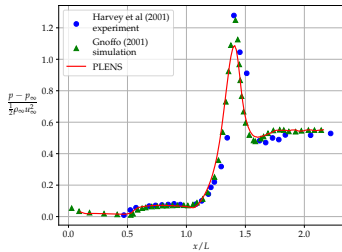
(b)  $St$

► Fine grid

- Secondary separation
  - ↪ bubble oscillations
  - ↪ divergence



(a) Surface plot of  $T$  with streamlines

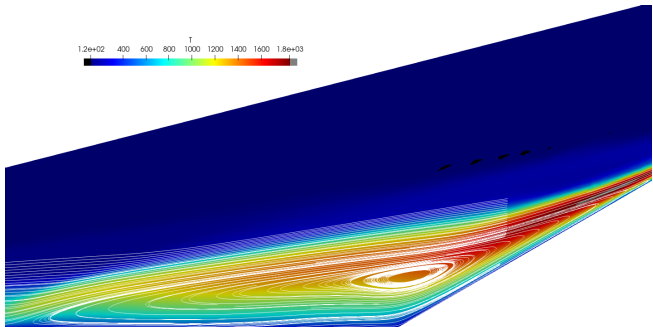


(b)  $c_p$

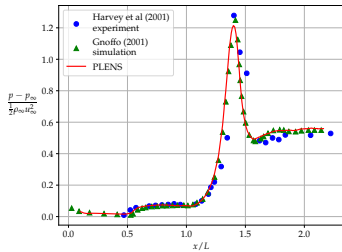
Figure: Counter: 1736

► Fine grid

- Secondary separation
  - ↪ bubble oscillations
  - ↪ divergence



(a) Surface plot of  $T$  with streamlines

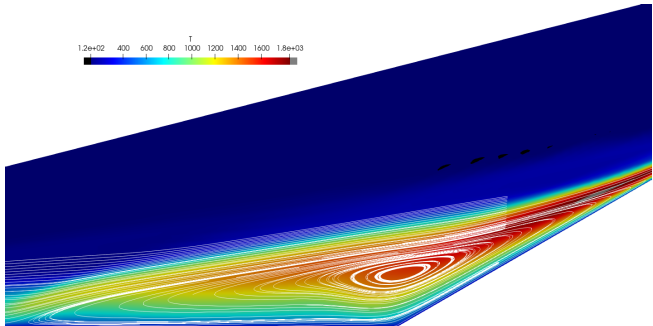


(b)  $c_p$

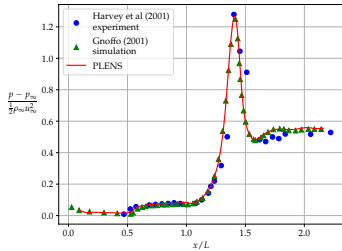
Figure: Counter: 1757

► Fine grid

- Secondary separation
  - ↪ bubble oscillations
  - ↪ divergence



(a) Surface plot of  $T$  with streamlines

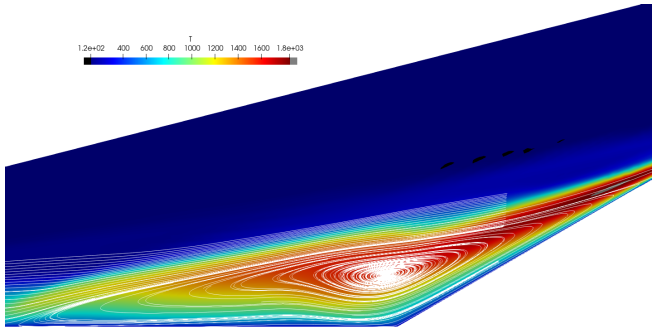


(b)  $c_p$

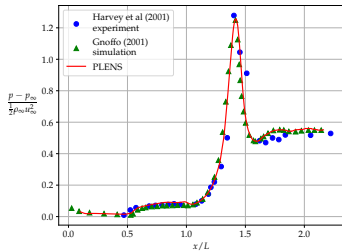
Figure: Counter: 1777

► Fine grid

- Secondary separation
  - ↪ bubble oscillations
  - ↪ divergence



(a) Surface plot of  $T$  with streamlines

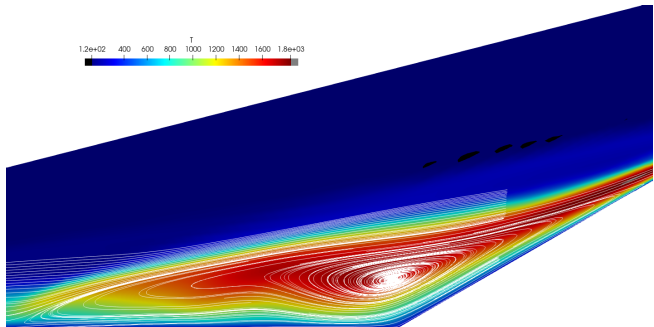


(b)  $c_p$

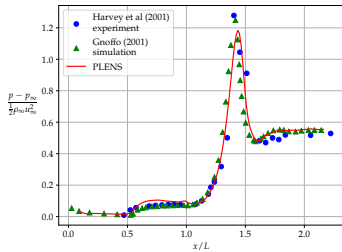
Figure: Counter: 1797

► Fine grid

- Secondary separation
  - ↪ bubble oscillations
  - ↪ divergence



(a) Surface plot of  $T$  with streamlines

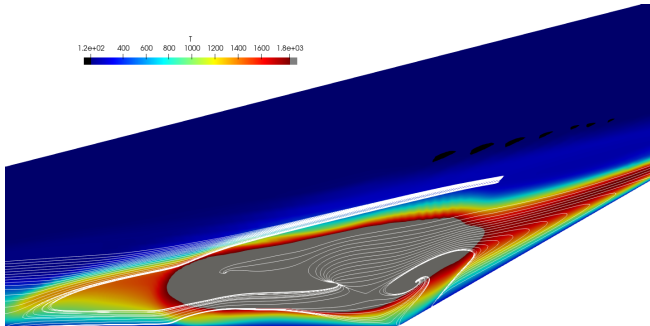


(b)  $c_p$

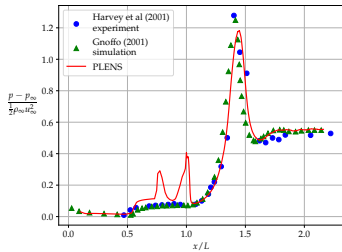
Figure: Counter: 1820

► Fine grid

- Secondary separation
  - ↪ bubble oscillations
  - ↪ divergence



(a) Surface plot of  $T$  with streamlines

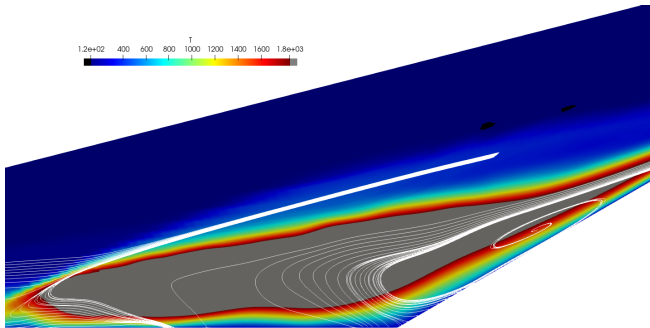


(b)  $c_p$

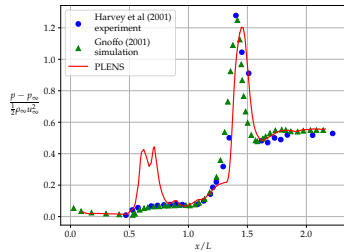
Figure: Counter: 1830

► Fine grid

- Secondary separation
  - ↪ bubble oscillations
  - ↪ divergence



(a) Surface plot of  $T$  with streamlines

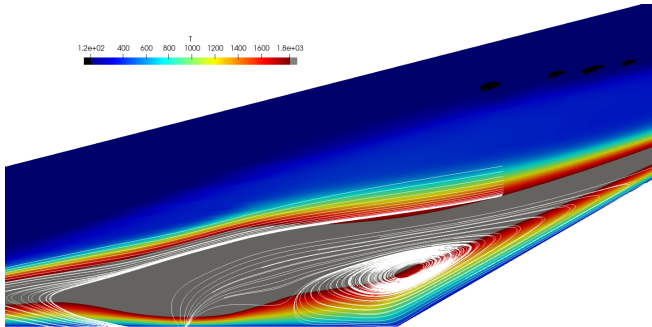


(b)  $c_p$

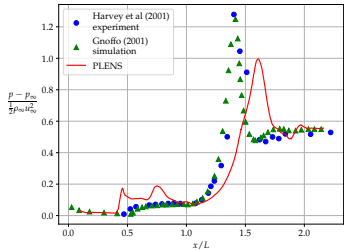
Figure: Counter: 1840

► Fine grid

- Secondary separation
  - ↪ bubble oscillations
  - ↪ divergence



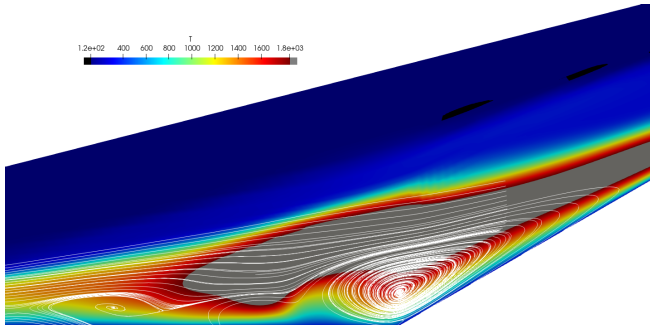
(a) Surface plot of  $T$  with streamlines



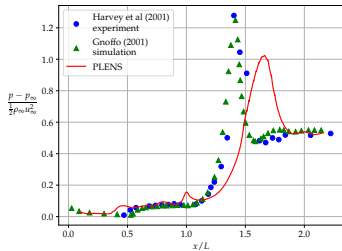
(b)  $c_p$

Figure: Counter: 1860

- ▶ Fine grid
  - Secondary separation
    - ↪ bubble oscillations
    - ↪ divergence
- ▶ Similar behaviour observed in HCEF Runs 8, 11 & 14
- ▶ Changing the numerical settings (CFL, flux scheme) gave no improvement



(a) Surface plot of  $T$  with streamlines

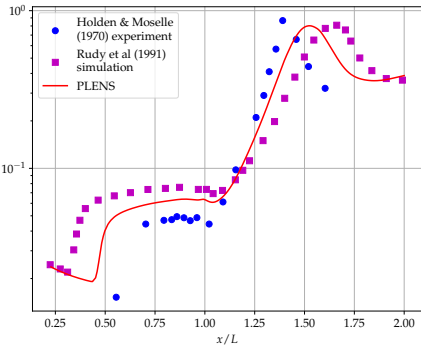
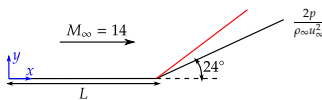


(b)  $c_p$

Figure: Counter: 1880

## ► Coarse grid (using $N = 2$ )

- Simulations over predict separation extent due to 3d effects [Rud+91]



## ► Fine grid

- Initially: results move closer to Rudy's
- Eventually: oscillations in separation bubble

Behaviour observed similar to that in HCEF Runs

# Conclusion and future work

## Conclusion

- ▶ Extended a subcell limiter to hypersonic regime
- ▶ Tested the modification on several cases in the regime  $6 \leq M_\infty \leq 14$
- ▶ Steady state divergence observed on fine grids at higher Mach numbers
- ▶ Explicit time integration might be the reason for this behaviour
  - Steady state convergence issues with explicit method reported in some FVM simulations too [CND01; RH10]

## Future work

- ▶ Study of SBLI control strategies in configurations of practical interest

## Appendix

## Reliable modelling?

- ▶ Chemistry: lack of experimental data at hypersonic flow conditions, extrapolation leads to poor results
- ▶ Turbulence
  - RANS: high uncertainty to RANS models used, inaccurate heat transfer results unless certain factors accounted for
    - Shock-turbulence interaction
    - Compressibility effects
  - LES, hybrid RANS-LES: "show promise"

## DG

- ▶ High order without increase in complexity?
  - Not worry about mesh structure/type/orientation etc.

## [Chi+19]'s results

### Cylinder case

- ▶ For a 3d tetrahedral element, number of DoFs per element is

$$\frac{(N+3)(N+2)(N+1)}{6} = {}^{N+3}C_3$$

Elements	
Coarse mesh	1320
Fine mesh	5280

- ▶  $Re_D = 376\,930$
- ▶  $M_\infty = 17.6$

$$St = \frac{q''_w}{\rho_\infty c_p u_\infty (T_{0\infty} - T_w)}$$

### Double cone case

- ▶  $Re = 140\,000\,m^{-1}$
- ▶ Mesh:  $192 \times 96$

## Advantages of [Hen+21]'s limiter

- ➊ Works on 3d curved (hexahedral) elements
- ➋ Limiter is more like a regulator rather than a switch
  - Most limiters act like switches: "do this in non-troubled cells, and do this in troubled cells"
  - This scheme does the same thing in all cells, but changes the value of  $\alpha$  accordingly
  - Not all troubled cells need to have high values of  $\alpha \implies$  high order contribution not completely disregarded in those cells
  - Some high order contribution can be retained in all cells if  $\alpha_{\max} < 1$
- ➌ The base algorithm has already been extended to turbulent flows [Lod+22] (advantage of split-flux formulation)
  - Split-form DGSEM is suited for turbulent flows (see next slide)

# Anti-aliasing [Win+18]

Issues in high order solutions of turbulent flows: numerical instability due to

① Insufficient dissipation

- Simulations generally do not fully “resolve” all scales
- Significantly higher energy at small scales

Solved by modelling small scales → LES

② Spectral methods use under-integration of nonlinear terms for efficiency

- Lead to aliasing driven instabilities
- Sometimes stability not possible even with de-aliasing
- Worse at high orders due to lesser inherent dissipation introduced by the scheme

One approach to solve this issue is the split-form DGSEM

Different forms of  $\mathbf{F}^\#$  give different stability properties:

$$\mathbf{F}_{\text{DG}}^\#(\mathbf{U}_a, \mathbf{U}_b) = \{\{\mathbf{F}(\mathbf{U})\}\}, \quad \mathbf{F}_{\text{Ch}}^\#(\mathbf{U}_a, \mathbf{U}_b) = \begin{bmatrix} \rho^{\ln} \{\{u\}\} \\ \rho^{\ln} \{\{u\}\}^2 + \hat{p} \\ \rho^{\ln} \{\{u\}\} \hat{h} \end{bmatrix}$$

where  $\{\{x\}\} := (x_a + x_b)/2$ ,  $x^{\ln} := (x_a - x_b)/\ln(x_a/x_b)$  and  $\beta := \rho/2p$

## Entropy/KE stability [FC13; Hen+21]

Entropy condition for a hyperbolic equation

$$\frac{\partial u}{\partial t} + \frac{\partial f}{\partial x} = 0 \quad (1)$$

requires existence of

- ① Convex function  $\eta(u)$
- ② Entropy flux  $q(u)$  satisfying  $\eta'f' = q'$

The entropy variables  $v = \frac{\partial \eta}{\partial u}$  contract Eq. (1) to

$$\frac{\partial \eta}{\partial t} + \frac{\partial q}{\partial x} = 0 \quad \text{in smooth regions}$$

$$\frac{\partial \eta}{\partial t} + \frac{\partial q}{\partial x} \leq 0 \quad \text{satisfied in distributional sense in discontinuous regions}$$

A scheme satisfies entropy stability if it obeys

$$\int_{x_1}^{x_2} \frac{\partial \eta}{\partial t} + q(x_2) - q(x_1) \leq 0$$

in a discrete sense

Section 3 of [Hen+21] shows that both  $R_{sf}^{HO}$  and  $R_{sc}^{LO}$  satisfy the discrete entropy inequality

## DGSEM-BR1 approach with entropy variables

From the abstract of [Gas+18]:

*... we prove that the BR1 scheme preserves the entropy stability of the recently developed entropy stable compressible Euler DGSEM discretization of ...*

However, we found that conservative variable gradients perform better in hypersonic cases

(hcef\_run9/trial2 diverged with entropy variables, while converged with conservative variables)

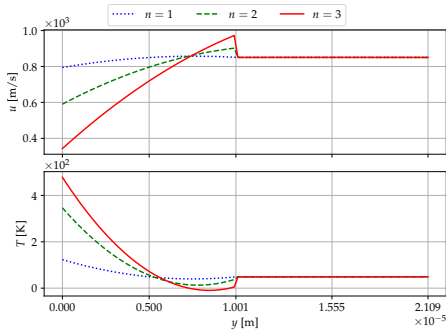
$$\Delta t_e = \text{CFL} \times \frac{1}{N^{1.5}} \min_{\text{Element nodes}} \left[ \frac{1}{\|\underline{\mathbf{J}}^{-1}\mathbf{u}\|_\infty + \frac{a}{h_e} + \frac{N^2 \nu}{h_e^2}} \right],$$

$$\Delta t = \min_{\text{Elements}} \Delta t_e,$$

$$\Delta t'_e = \min_{n \in \text{Neighbors}} \{\Delta t_e, \tau_n \Delta t_n, \tau_g \Delta t\}$$

## Hypersonic extension

- ▶ Crash occurs right in the beginning when flow starts developing from IC
- ▶ IC is generally freestream condition  $\Rightarrow$  very high velocity difference
- ▶ Diffusive flux is the major contributor here, since any contact resolving advective flux scheme would preserve the IC



- ▶ The wall correction is required since the value of  $\alpha$  doesn't stay high for sufficiently long time
- ▶ In steady state,  $\alpha_d \neq 0$  only at LE

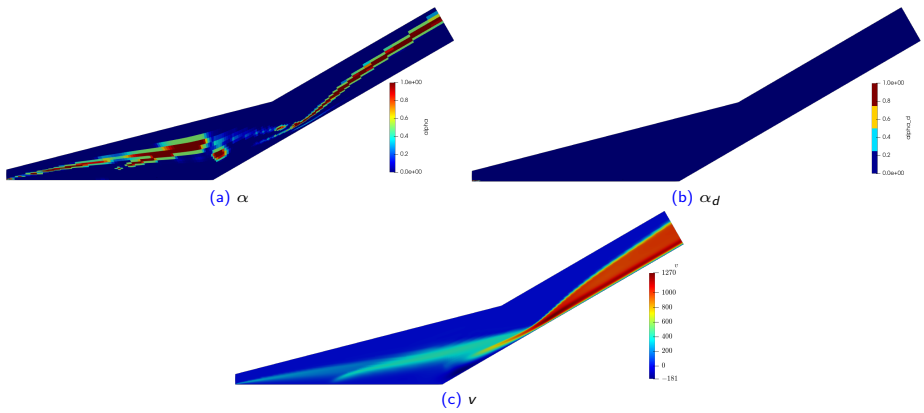


Figure: Converged results of HCEF Run 9

## Jacob's case

- ▶  $T_w = T_\infty = 222 \text{ K}$ ,  $M_\infty = 2$ ,  $\rho_\infty = 0.004\ 04 \text{ kg m}^{-3}$
- ▶  $x \in [0, 1]$ ,  $20 \times 20$  cells,  $N = 4$ , CFL 0.5, RK4
- ▶ Time accurate simulation up to 8 ms
- ▶ Result compared at  $x = 0.9164 \text{ m}$
- ▶ The reference solution is not Jacob's computation but from a "spectrally accurate BL code"<sup>1</sup>

---

<sup>1</sup>Pruett & Streett; A spectral collocation method for compressible, non-similar boundary layers; 1991

## Degrez's case

- ▶  $p_0 = 10.7 \text{ kPa}$ ,  $T_0 = 293 \text{ K}$ ,  $M_\infty = 2.15$
- ▶  $X_{\text{sh}} = 80 \text{ mm}$ ,  $N = 4$ ,  $30 \times 22$  cells, 18 DoFs within unperturbed BL at  $x = X_{\text{sh}}$
- ▶  $N = 4$ , RK4, CFL 0.5

## Lewis' cases

- ▶  $M_\infty = 6.06$ ,  $L = 6.35 \text{ cm}$
- ▶  $T_0$ ,  $p_0$  not given; [Car73] uses  $T_\infty = 48.89 \text{ K}$  for flat plate case and compares them with [LKL68] flat plate experiments
- ▶ Since the same tunnel is used for compression corner experiments too, this value of  $T_\infty$  is used
- ▶  $p_\infty$  is calculated using  $\text{Re}_L$
- ▶ [LKL68] mention that  $\text{Re}_L$  was changed keeping  $T_0$  (and hence  $T_\infty$ ) fixed and changing  $p_0$  (and hence  $p_\infty$ )
- ▶  $5\Delta y_w^2/\nu_\infty \approx 0.4 \mu\text{s}$
- ▶ [Car73] uses a 2nd order FDM

**Table:** Mesh details for  $\text{Re}_L = 1.5 \times 10^5$ , adiabatic wall case

Mesh #	Grid	$\Delta y_w$ ( $\mu\text{m}$ )	$\text{Re}_L \Delta y_w / L$
1	$135 \times 60$	10	24
2	$180 \times 80$	7.5	18
3	$225 \times 80$	7.5	18
4	$180 \times 100$	5	12

# HCEF Runs

Run #	$\rho_\infty$ (kg m <sup>-3</sup> )	$u_\infty$ (m s <sup>-1</sup> )	$T_\infty$ (K)	$M_\infty$	$Re_u$ (m <sup>-1</sup> )	$T_w$ (K)
8	0.001 206	2667	132.8	11.35	359 600	296.7
9	0.000 845	2566	121.1	11.44	264 830	296.7
11	0.000 507	2609	128.9	11.27	152 010	297.2
14	0.000 794	2432	156.1	9.55	185 800	295.6

## ► Coarse grid

- ①  $136 \times 45$
- ②  $\Delta y_w = 50 \mu\text{m} \implies Re_u \Delta y_w = 13$
- ③  $5\Delta y_w^2 / \nu_\infty \approx 0.7 \mu\text{s}$

## ► Fine grid

- ①  $136 \times 64$
- ②  $\Delta y_w = 30 \mu\text{m} \implies Re_u \Delta y_w = 7.8$

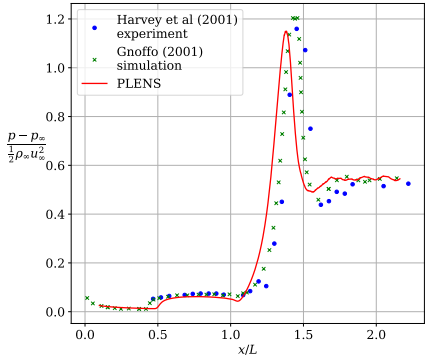
## ► Gnoffo's result

- ① LAURA
- ② Roe flux and Yee's TVD 2nd order formulation (minmod limiter)
- ③ Point-implicit relaxation (implicit time stepping scheme)
- ④ TLNS formulation of viscous fluxes

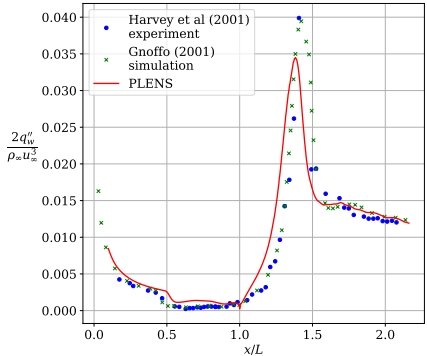
*This formulation includes all but the cross derivative terms ...*

- ⑤ Mesh: not mentioned

Trial #	Grid size	$\Delta y_w$ ( $\mu\text{m}$ )	Notes	Observation
1	$180 \times 64$	30	HCEF Run 14's trial 1 mesh	Oscillated
2	$136 \times 45$	50		Best result
3	$136 \times 64$	30	Both number of cells and $\Delta y_w$ changed; tried using Rusanov flux too	Oscillated
4	$136 \times 45$	30	Only $\Delta y_w$ changed compared to trial 2	No change in results
5	$136 \times 55$	30	$\Delta y_w$ unchanged compared to trial 4, only resolution in top block increased	Oscillated
6	$180 \times 55$	30	Only resolution in $x$ increased compared to trial 5	Oscillated



(a)  $c_p$



(b)  $St$

**Figure:** HCEF Run 8, best result (validation/hcef\_run8/group7/trial4/result)

For HCEF Runs 11 & 14, all meshes tried were “fine” ( $180 \times 64$ ). No “coarse” solution was tried. All cases diverged.

## Hung's case

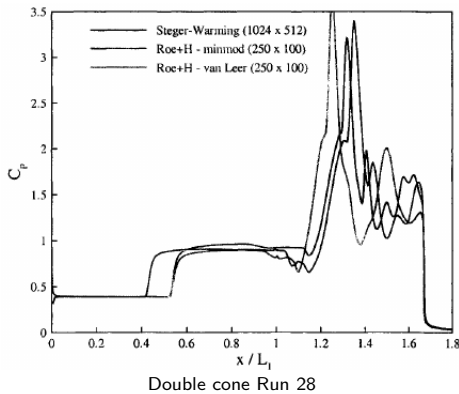
- ▶  $p_\infty = 10 \text{ Pa}$ ,  $T_\infty = 72.2 \text{ K}$ ,  $M_\infty = 14.1$ ,  $\text{Re}_L = 1.04 \times 10^5$ ,  $L = 0.4389 \text{ m}$
- ▶  $T_w = 297.22 \text{ K}$
- ▶  $5\Delta y_w^2/\nu_\infty \approx 0.6 \mu\text{s}$
- ▶ [Rud+91]'s paper uses 4 different commercial codes: CFL3D, USA-PG2, NASCRIN, LAURA

Mesh #	Grid size	$\Delta y_w$ ( $\mu\text{m}$ )	$\text{Re}_L \Delta y_w / L$
1	$131 \times 44$	300	71
2	$195 \times 66$	207	49

## Divergence with explicit methods

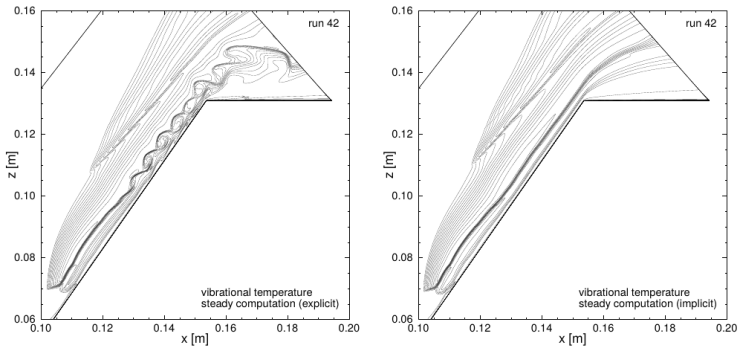
- ▶ Difficult to find many evidences since people seldom use explicit methods for the cases considered
- ▶ Candler, Nompelis, and Druguet [CND01]

*It should be noted that the Steger-Warming calculation is performed on a much finer grid ( $1024 \times 512$ ) than the other two results ( $250 \times 100$ ), because of difficulties with obtaining a converged solution with an explicit method.*



► Reimann and Hannemann [RH10]

Although not observed in the experiments, this shear layer becomes unstable in the numerical simulations. Only in the lower Reynolds number case the more dissipative time integration of the implicit scheme is able to stabilize the laminar shear layer and results in a steady state solution. As depicted in... the explicit [3 stage] Runge-Kutta scheme shows for this case an unstable shear layer despise[sic] all techniques activated to converge to a steady state solution. In case of the higher Reynolds number of run 40 even the implicit scheme does not provide a steady state solution. Therefore, a time accurate simulation was conducted for run 40.



Double cone Run 42

- ▶ Hypersonic CFD plays crucial role in scramjet design
- ▶ Scramjet inlet simulations are one primary building block for the design
- ▶ High order, low dissipation simulations may offer an efficient alternative for scramjet inlet simulations
  - Lesser sensitivity to turbulence modelling  $\implies$  reliable results
  - Lesser cost and/or memory requirement for the same accuracy
- ▶ The method proposed here can be used for scramjet simulations since  $M_\infty \leq 6$  in these cases

# References |

- [Arn+21] Daniel Arndt et al. "The deal.II Library, Version 9.3". In: *Journal of Numerical Mathematics* 29.3 (2021), pp. 171–186.
- [BD10] Garrett E Barter and David L Darmofal. "Shock capturing with PDE-based artificial viscosity for DGFEM: Part I. Formulation". In: *Journal of Computational Physics* 229.5 (2010), pp. 1810–1827.
- [BM12] Nicholas Burgess and Dimitri Mavriplis. "Computing Shocked Flows with High-order Accurate Discontinuous Galerkin Methods". In: *42nd AIAA Fluid Dynamics Conference and Exhibit*. 2012.
- [BM13] Michael J Brazell and Dimitri J Mavriplis. "3D mixed element discontinuous Galerkin with shock capturing". In: *21st AIAA Computational Fluid Dynamics Conference*. 2013, p. 3064.
- [Boh+20] Marvin Bohm et al. "An entropy stable nodal discontinuous Galerkin method for the resistive MHD equations. Part I: Theory and numerical verification". In: *Journal of Computational Physics* 422 (2020), p. 108076.
- [BRG13] Ankush Bhatia, Subrata Roy, and Ryan Gosse. "2-D hypersonic non-equilibrium flow simulation using rp adaptive time-implicit discontinuous Galerkin method". In: *51st AIAA Aerospace Sciences Meeting including the New Horizons Forum and Aerospace Exposition*. 2013, p. 302.
- [Can15] Graham Candler. "Rate-dependent energetic processes in hypersonic flows". In: *Progress in Aerospace Sciences* 72 (2015), pp. 37–48.
- [Car73] James E Carter. "Numerical solutions of the supersonic, laminar flow over a two-dimensional compression corner". In: *Proceedings of the Third International Conference on Numerical Methods in Fluid Mechanics*. Springer. 1973, pp. 69–78.
- [Chi+19] Eric J. Ching et al. "Shock capturing for discontinuous Galerkin methods with application to predicting heat transfer in hypersonic flows". In: *Journal of Computational Physics* 376 (2019), pp. 54–75.

## References II

- [CKS12] Bernardo Cockburn, George E Karniadakis, and Chi-Wang Shu. "The Development of Discontinuous Galerkin Methods". In: *Discontinuous Galerkin methods: theory, computation and applications*. Ed. by Bernardo Cockburn, George E Karniadakis, and Chi-Wang Shu. Vol. 11. Springer Science & Business Media, 2012. Chap. 1.
- [CMT09] Graham Candler, Dimitri Mavriplis, and Loretta Trevino. "Current status and future prospects for the numerical simulation of hypersonic flows". In: *47th AIAA Aerospace Sciences Meeting Including the New Horizons Forum and Aerospace Exposition*. 2009, p. 153.
- [CND01] Graham Candler, Ioannis Nompelis, and Marie-Claude Druguet. "Navier-Stokes Predictions of Hypersonic Double-Cone and Cylinder-Flare Flow Fields". In: *39th Aerospace Sciences Meeting and Exhibit*. 2001, p. 1024.
- [DCN05] Marie-Claude Druguet, Graham V Candler, and Ioannis Nompelis. "Effects of numerics on Navier-Stokes computations of hypersonic double-cone flows". In: *AIAA journal* 43.3 (2005), pp. 616–623.
- [FC13] Travis C Fisher and Mark H Carpenter. "High-order entropy stable finite difference schemes for nonlinear conservation laws: Finite domains". In: *Journal of Computational Physics* 252 (2013), pp. 518–557.
- [Fra+12] Sarah Frauholz et al. "Numerical simulation of hypersonic air intake flow in scramjet propulsion using a mesh-adaptive approach". In: *18th AIAA/3AF International Space Planes and Hypersonic Systems and Technologies Conference*. 2012, p. 5976.
- [Gai15] Datta V Gaitonde. "Progress in Shock Wave/Boundary Layer Interactions". In: *Progress in Aerospace Sciences* 72 (2015), pp. 80–99.
- [Gao+19] Song Gao et al. "A finite element solver for hypersonic flows in thermo-chemical non-equilibrium, Part II". In: *International Journal of Numerical Methods for Heat & Fluid Flow* (2019).

## References III

- [Gas+18] Gregor J Gassner et al. "The BR1 scheme is stable for the compressible Navier–Stokes equations". In: *Journal of Scientific Computing* 77.1 (2018), pp. 154–200.
- [Gre+10] Christopher J Greenshields et al. "Implementation of semi-discrete, non-staggered central schemes in a colocated, polyhedral, finite volume framework, for high-speed viscous flows". In: *International Journal for Numerical Methods in Fluids* 63.1 (2010), pp. 1–21.
- [GS98] Sigal Gottlieb and Chi-Wang Shu. *Total Variation Diminishing Runge-Kutta schemes*. Tech. rep. 221. Mathematics of computation of the American Mathematical Society, Jan. 1998, pp. 73–85.
- [Hen+21] Sebastian Hennemann et al. "A provably entropy stable subcell shock capturing approach for high order split form DG for the compressible Euler equations". In: *Journal of Computational Physics* 426 (2021), p. 109935.
- [Hol+18] Kevin R Holst et al. "High-Order Simulations of Shock Problems using HPCMP CREATE (TM)-AV Kestrel COFFE". In: *2018 AIAA Aerospace Sciences Meeting*. 2018, p. 1301.
- [HW07] Jan S Hesthaven and Tim Warburton. *Nodal discontinuous Galerkin methods: algorithms, analysis, and applications*. Springer Science & Business Media, 2007.
- [KC10] Benjamin Kirk and Graham F. Carey. "Validation Studies of Fully Implicit, Parallel Finite Element Simulations of Laminar Hypersonic Flows". In: *AIAA Journal* 48.6 (2010), pp. 1025–1036.
- [KCL00] Christopher A. Kennedy, Mark H. Carpenter, and R.Michael Lewis. "Low-storage, explicit Runge–Kutta schemes for the compressible Navier–Stokes equations". In: *Applied Numerical Mathematics* 35.3 (2000), pp. 177–219.
- [Kir+14] Benjamin Kirk et al. "Modeling hypersonic entry with the fully-implicit Navier–Stokes (FIN-S) stabilized finite element flow solver". In: *Computers & Fluids* 92 (2014), pp. 281–292.
- [Kni+12] Doyle Knight et al. "Assessment of CFD capability for prediction of hypersonic shock interactions". In: *Progress in Aerospace Sciences* 48-49 (2012), pp. 8–26.

## References IV

- [Kni+17] Doyle Knight et al. "Assessment of predictive capabilities for aerodynamic heating in hypersonic flow". In: *Progress in Aerospace Sciences* 90 (2017), pp. 39–53.
- [LD07] Xin Liu and Xiaogang Deng. "Application of High-Order Accurate Algorithm to Hypersonic Viscous Flows for Calculating Heat Transfer Distributions". In: *45th AIAA Aerospace Sciences Meeting and Exhibit*. 2007.
- [LKL68] John E Lewis, Toshi Kubota, and Lester Lees. "Experimental investigation of supersonic laminar, two-dimensional boundary-layer separation in a compression corner with and without cooling.". In: *AIAA Journal* 6.1 (1968), pp. 7–14.
- [Lod+22] Diego Lodatare et al. "An entropy-stable discontinuous Galerkin approximation of the Spalart–Allmaras turbulence model for the compressible Reynolds Averaged Navier–Stokes equations". In: *Journal of Computational Physics* 455 (2022), p. 110998.
- [Maw+06] M K Mawlood et al. "Solution of Navier-Stokes equations by fourth-order compact schemes and AUSM flux splitting". In: *International Journal of Numerical Methods for Heat and Fluid Flow* 16.1 (2006), pp. 107–120.
- [Men+14] Gianmarco Mengaldo et al. "A guide to the implementation of boundary conditions in compact high-order methods for compressible aerodynamics". In: *AIAA AVIATION 2014 -7th AIAA Theoretical Fluid Mechanics Conference*. 2014.
- [RH10] Bodo Reimann and Volker Hannemann. "Numerical investigation of double-cone and cylinder experiments in high enthalpy flows using the DLR TAU code". In: *48th AIAA Aerospace Sciences Meeting Including the New Horizons Forum and Aerospace Exposition*. 2010, p. 1282.
- [Rud+91] David H Rudy et al. "Computation of laminar hypersonic compression-corner flows". In: *AIAA Journal* 29.7 (1991), pp. 1108–1113.

## References V

- [Seg+19] Jory Seguin et al. "A finite element solver for hypersonic flows in thermo-chemical non-equilibrium, Part I". In: *International Journal of Numerical Methods for Heat & Fluid Flow* (2019).
- [SNC14] Alan Schwing, Ioannis Nompelis, and Graham Candler. "Parallelization of unsteady adaptive mesh refinement for unstructured Navier-Stokes solvers". In: *7th AIAA Theoretical Fluid Mechanics Conference*. 2014, p. 3080.
- [SZH10] Yiqing Shen, Gecheng Zha, and Manuel Huerta. "Simulation of Hypersonic Shock Wave/Boundary Layer Interaction Using High Order WENO Scheme". In: *48th AIAA Aerospace Sciences Meeting Including the New Horizons Forum and Aerospace Exposition*. 2010.
- [Win+18] Andrew R. Winters et al. "A comparative study on polynomial dealiasing and split form discontinuous Galerkin schemes for under-resolved turbulence computations". In: *Journal of Computational Physics* 372 (2018), pp. 1–21.
- [Zha+11] Xiaohui Zhao et al. "Some Applications of WCNS-E-5 on Shock-Wave/Boundary-Layer Interactions and Aerodynamic Heating Prediction in Hypersonic Flows". In: *20th AIAA Computational Fluid Dynamics Conference*. 2011, p. 3858.